Materials Letters 308 (2022) 131244

Contents lists available at ScienceDirect

Materials Letters

journal homepage: www.elsevier.com/locate/matlet

Implanted gallium impurity detection in silicon by impedance spectroscopy

David Tetelbaum [a,*], Alena Nikolskaya [a], Mikhail Dorokhin [a], Valery Vasiliev [a], Dmitriy Smolyakov [b], Anna Lukyanenko [b,c], Filipp Baron [b], Anton Tarasov [b,c]

[a] Research Institute of Physics and Technology, Lobachevsky University, 23/3 Gagarina Avenue, Nizhny Novgorod, 603022, Russia
[b] Kirensky Institute of Physics, 50 st. Akademgorodok, Krasnoyarsk 660036, Russia
[c] Institute of Engineering Physics and Radio Electronics, Siberian Federal University, 79 Svobodny pr., Krasnoyarsk 660041, Russia

ARTICLE INFO

Keywords:
Silicon
Ion implantation
Impedance spectroscopy
Impurity centers
Energy levels
Ion channeling

ABSTRACT

The results of determining the energy levels of boron-doped silicon implanted with gallium ions by impedance spectroscopy are reported. In the as-implanted sample the boron level remains the same and a second level appears close to the Ga-level reported in literature. In the sample annealed at 1000 °C, two levels are observed neither of which corresponds to the literature values for boron and gallium. It is assumed that in the as-implanted sample this method detects levels of gallium atoms located at a depth where ions penetrate due to the channeling effect, since a large concentration of defects at shallower depths does not allow detection of energy levels due to the Fermi level pinning. Explaining the results for the sample annealed after implantation requires additional research. The main result of this work is to establish the possibility of detecting impurity levels in ion-implanted silicon by impedance spectroscopy even in the absence of subsequent annealing.

1. Introduction

Modern electronics is placing ever higher and more diverse demands on the quality and parameters of semiconductor devices. An example of the latter is beta-voltaic cells [1]. Changing or adding an impurity and precise control of its profile in such structures is one of the ways to manipulate the transport properties of semiconductors, thus, achieving the highest values of efficiency. To achieve the latter requirements some additional research, in particular, the determination of the impurity energy levels is of great importance. Ion implantation is the most effective way to introduce impurities of the desired type with a precise concentration and profile control [2]. In the absence of annealing the concentration of implantation-induced electrically active defects is several orders of magnitude higher than the concentration of the initial and implanted impurities. In this case, the Hall effect measurements along with the other stationary methods do not provide information about the electrical state of the impurities located in implanted layer [3]. In the present work, using low-dose Ga^+ implantation in silicon, as the example, it is shown that such a challenge can be successfully solved by applying the impedance spectroscopy method [4].

2. Materials and methods

Impedance spectroscopy (IS) is based on the study of frequency and temperature dependences of the real part of impedance *(R)*. It allows determining the energy levels of impurity centers in semiconductors. The method is universal and applicable to various materials, including nanostructures (see for example [5,6]). In this work, the possibility of applying this method to ion-doped silicon samples, including as-implanted ones, at low doses of heavy ion irradiation was investigated. A boron-doped ($p \approx 10^{12}$ cm^{-3}) 350 μm thick p-Si wafer was exposed to Ga^+ with an energy E = 80 keV and a dose $F = 1{\cdot}10^{12}$ cm^{-2}. The ion beam direction was orthogonal to the surface of the sample, i.e. no special measures were used to suppress the channeling effect. Some samples were post-annealed at 1000 °C (15 min) in dry N_2 at 312 Pa and the humidity corresponding to the dew-point −39.3 °C. The annealing chamber was pre-annealed and purged with N_2. After switching on the heating lamps the temperature was raised to 1000 °C during 40 sec; the cooling rate after switching off the lamps was 7°/s from 1000 to 500 °C, and 2°/s from 500 °C to room temperature. Schottky back-to-back diodes were prepared using EPO-TEK H20S silver two-component epoxy glue deposited to the front and back sides of the sample as ~1 mm^2 contacts (see the inset in Fig. 1a). To measure temperature dependences of the real *R(T)* and imaginary *X(T)* parts of impedance, the sample was

---

* Corresponding author.
E-mail address: tetelbaum@phys.unn.ru (D. Tetelbaum).

https://doi.org/10.1016/j.matlet.2021.131244
Received 1 July 2021; Received in revised form 2 November 2021; Accepted 3 November 2021

cooled in a helium cryostat. R and X were independently measured with an E4980A precision LCR-meter during heating the sample from 4.2 K to 300 K. An alternating voltage $V_{ac} = 0.1$ V with frequencies (f) from 20 Hz to 2 MHz was applied to the sample as shown in the inset of Fig. 1a.

3. Results and discussion

The $R(T)$ for initial, as-implanted and post-implantation-annealed samples were measured (Fig. 1). The temperature curves $R(T)$ reveal peculiarities in the form of peaks (T_m), which position depends on frequency f (Fig. 1a) observed in all samples. This behavior indicates the presence of a thermally activated energy state in the band-gap and the peaks arise due to the process of emission/capture of the charge carrier into/from the bands [7]. This process depends on the frequency of the AC voltage and the position of the energy level with respect to the Fermi level, which, in turn, depends on the temperature.

For clarity, the recharge process under the action of AC voltage is schematically shown in Fig. 2 for homogeneously doped p-Si at a temperature sufficient to cross the Fermi level with the energy level of the state detected. This temperature corresponds to T_m, which is the temperature of the $R(T)$ maximum, i.e. where the peak is observed (Fig. 1a). Thus, T_m will be different for different frequencies, as one may observe the peak position changes with the frequency.

According to [8], the approximate relationship between $\omega = 2\pi f$ and T_m is:

$$\omega = 2BN\exp(-E/kT_m) \tag{1}$$

where B is the capture coefficient of carriers, N – concentration of trapping centers, E – energy level, k – Boltzmann constant. The value of E is determined from the slope of the linear $\ln(\omega)$ vs. $1/T_m$ dependence. As can be seen from Fig. 3, the dependences of $\ln(\omega)$ on $1/T_m$ are well described by (1) for all three samples. The single maximum is observed for the initial sample (Fig. 1b) for which $E = 42.2$ meV. This value is very close to the boron level data ($E = 44$ meV) [9]. It is interesting that we managed to detect an impurity with concentration as small as $\sim 10^{12}$ cm^{-3}.

The $R(T)$ dependence for as-implanted sample shown at Fig. 1b represent two peaks. Plotting the dependence of $\ln(\omega)$ on $1/T_m$ (Fig. 3) allows attributing one of these peaks to the boron level ($E = 42.2$ meV). Another peak ($E = 69.4$ meV) can be interpreted as the gallium level for which the reference value is 73 meV [9]. Thus, the possibility of detecting the center associated with implanted atoms even without annealing was shown. In addition, it can be seen from the experiment that the initial boron impurity did not change its properties.

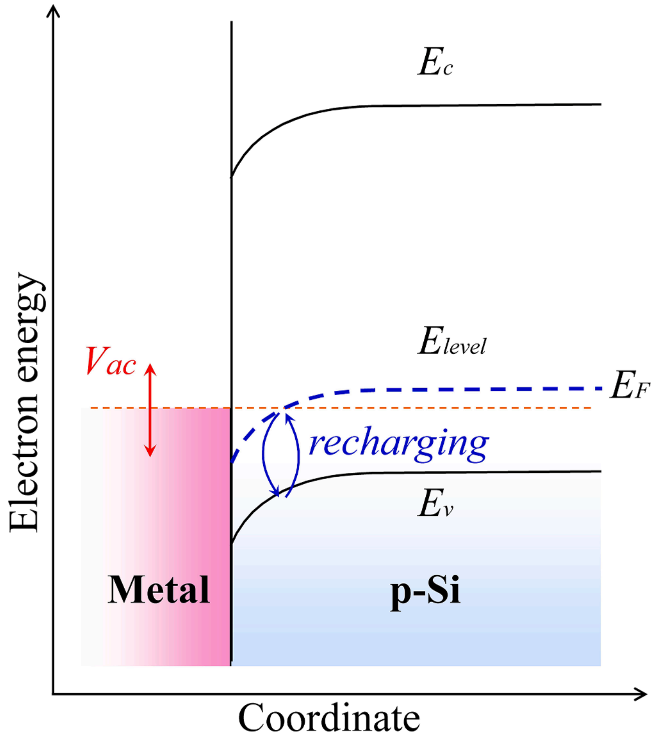

Fig.2. Energy diagram explaining the process of recharging of the acceptor level (E_{level}) for homogeneously doped p-Si. E_C and E_v – edges of the C- and V-bands, E_F - Fermi level, V_{ac} - alternating voltage. The energy diagram for as-implanted samples can be found in the "Supplementary materials" section Fig. S2.

We emphasize that such results are not trivial. The Fermi level in the implanted silicon should be pinned near the middle of the bandgap [10]. According to SRIM calculations [11] the concentration of implantation induced defects at the maximum of the Ga distribution exceeds 10^{17} cm^{-3}. Although not all of these defects survive at room temperature, for the depths corresponding to the ranges of unchannelled ions penetration, the Fermi level without post-implantation-annealing should maintain its position near the middle of the bandgap. This means that the impurity levels in that depth could not be determined by the method applied. Therefore, we suggest that the levels revealed in the experiment

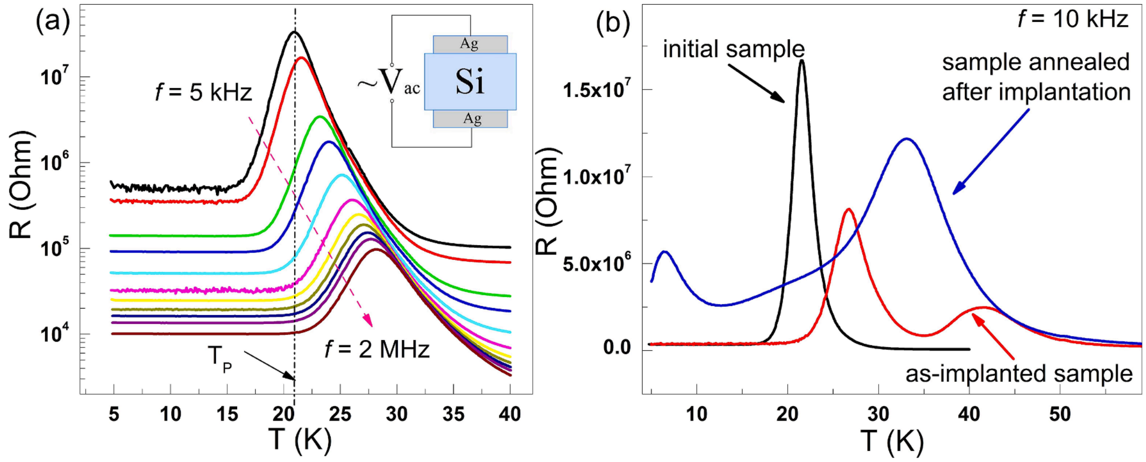

Fig.1. (a) The temperature dependence of R - real part of impedance at various frequencies f for the initial (virgin) sample, dependencies for as-implanted and post-implantation-annealed samples are shown in "Supplementary materials" Fig. S1; (b) the temperature dependence of R at 10 kHz for the initial, as-implanted and post-implantation-annealed samples. The values of the used f are: 5 kHz, 10 kHz, 50 kHz, 100 kHz, 250 kHz, 500 kHz, 750 kHz, 1 MHz, 1.25 MHz, 1.5 MHz, 2 MHz. The inset in Fig. 1a shows a schematic of the impedance measurement.

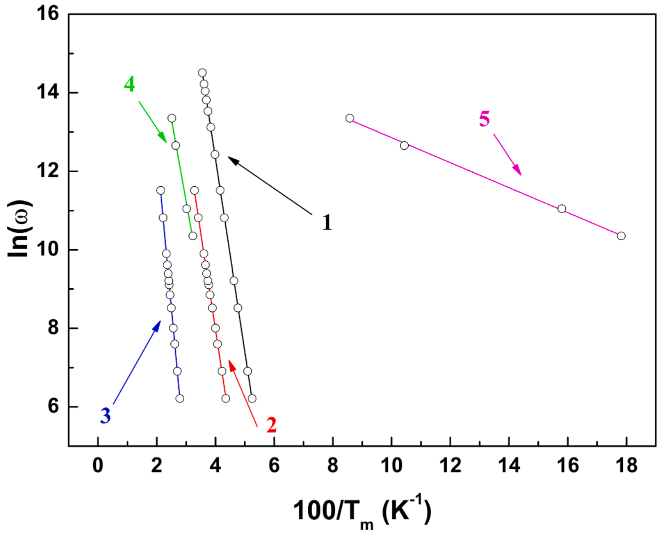

Fig.3. Dependence of ln(ω) on $1/T_m$ for initial (1), as-implanted (2, 3) and post-implantation-annealed (4, 5) samples.

for the as-implanted sample refer to *deeper* layers where Ga^+ ions penetrate due to the *channeling effect* [3]. Indeed, in general, a small fraction of the implanted Ga^+ enters the channels and have a certain chance to replace lattice sites [11], thereby becoming the acceptor centers. Since the penetration depth for channeled Ga^+ ions is much larger than the maximum impurity concentration depth, the concentration of radiation defects in this region is not high enough to pin the Fermi level and, thus, the method we applied allows one to determine the levels of both initial and implanted impurities.

In the implanted sample *after annealing* at 1000 °C when almost all defects are annihilated [3], two peaks are again observed at $R(T)$ dependence (Fig. 1b), however, their positions are shifted (Fig. 3). These energy levels are found to be 2.7 and 36.1 meV, i.e. significantly lower than the values reported in literature. This result is not fully clear. Since the Fermi level is no longer pinned for annealed sample, the measurements reveal the levels of impurities located at depths where the majority of implanted atoms (i.e. unchannelled) are located. Therefore, the results obtained for annealed sample need to be explored further.

4. Conclusions

Using gallium ions as an example we found that the impedance spectroscopy method makes it possible to determine the levels of implanted impurity atoms even in the absence of post-implantation annealing. It can be expected that optimization of the channeling conditions will increase the fraction of implanted ions contributing to the signal from energy levels in as-implanted samples. This is important for the implantation technology of some devices such as beta-voltaic cells.

CRediT authorship contribution statement

David Tetelbaum: Conceptualization, Investigation, Writing – original draft, Supervision. **Alena Nikolskaya:** Formal analysis, Writing - review & editing. **Mikhail Dorokhin:** Validation, Formal analysis. **Valery Vasiliev:** Investigation. **Dmitriy Smolyakov:** Investigation, Data curation. **Anna Lukyanenko:** Investigation. **Filipp Baron:** Validation, Writing - review & editing. **Anton Tarasov:** Formal analysis, Investigation, Data curation, Visualization, Writing - review & editing.

Declaration of Competing Interest

The authors declare that they have no known competing financial interests or personal relationships that could have appeared to influence the work reported in this paper.

Acknowledgements

This study was supported by the Russian Foundation for Basic Research (grant No. 20-42-243007), Ministry of Science and Higher Education of the Russian Federation (project No. 075-03-2020-191/5), as well as the Government of the Russian Federation within the framework of the Megagrant for the creation of world-class laboratories (No. 075-15-2019-1886).

Appendix A. Supplementary data

Supplementary data to this article can be found online at https://doi.org/10.1016/j.matlet.2021.131244.

References

[1] P. Rappaport, The electron-voltaic effect in p-n junctions induced by beta-particle bombardment, Phys. Rev. 93 (1954) 246, https://doi.org/10.1103/PhysRev.93.246.2.

[2] M.I. Current, Ion implantation for fabrication of semiconductor devices and materials, Ind. Accel. Their Appl. (2012), https://doi.org/10.1142/9789814307055_0002.

[3] H. Ryssel, I. Ruge, in: Ion Implantation, John Wiley & Sons Ltd., Hoboken, 1986, https://doi.org/10.1002/sia.740100409.

[4] E. Barsoukov, J.R. Macdonald, in: Impedance Spectroscopy: Theory, Experiment, and Applications, second ed., Wiley, New Jersey, 2005 https://doi.org/10.1002/0471716243.

[5] N.V. Volkov, A.S. Tarasov, E.V. Eremin, A.V. Eremin, S.N. Varnakov, S. G. Ovchinnikov, Frequency-dependent magnetotransport phenomena in a hybrid Fe/SiO 2/p-Si structure, J. Appl. Phys. 112 (12) (2012) 123906, https://doi.org/10.1063/1.4769788.

[6] Y.V. Knyazev, A.S. Tarasov, M.S. Platunov, A.L. Trigub, O.A. Bayukov, A. I. Boronin, L.A. Solovyov, E.V. Rabchevskii, N.N. Shishkina, A.G. Anshits, Structural and electron transport properties of $CaFe_2O_4$ synthesized in air and in helium atmosphere, J. Alloys Compd. 820 (2020) 153073, https://doi.org/10.1016/j.jallcom.2019.153073.

[7] A.R. Peaker, V.P. Markevich, J. Coutinho, Tutorial: junction spectroscopy techniques and deep-level defects in semiconductors, J. Appl. Phys. 123 (16) (2018) 161559, https://doi.org/10.1063/1.5011327.

[8] D.L. Losee, Admittance spectroscopy of impurity levels in Schottky barriers, J. Appl. Phys. 46 (5) (1975) 2204–2214, https://doi.org/10.1063/1.321865.

[9] S.M. Sze, K.K. Ng, Physics of Semiconductor Devices, in: Simon M. Sze, Kwok K. Ng (Eds.), Phys. Semicond. Devices, third ed., Wiley-Interscience, New Jersey, 2007.

[10] V.N. Brudnyĭ, N.G. Kolin, L.S. Smirnov, The model of self-compensation and pinning of the Fermi level in irradiated semiconductors, Semiconductors 41 (9) (2007) 1011–1020, https://doi.org/10.1134/S1063782607090023.

[11] J.F. Ziegler, M.D. Ziegler, J.P. Biersack, SRIM - the stopping and range of ions in matter, Nucl. Instrum. Methods Phys. Res. Sect. B Beam Interact. with Mater. Atoms. 268 (2010) 1818–1823, https://doi.org/10.1016/j.nimb.2010.02.091.